International Journal on Recent and Innovation Trends in Computing and Communication ISSN: 2321-8169
Volume: 4 Issue: 7 296 - 302

Optimization and Design Numerical Modeling and Advances in Fabrication Technologies to Optical Performance

Nadeem Khargan Alhareeb
Thiqar University
Biomedical Engineering department
Nassiriyiah,Iraq
nadeemkhargan@ymail.com

***Abstract*—**Photonic crystals and Nano photonics have received a great deal of attention over the last decade, largely due to improved numerical modeling and advances in fabrication technologies. To this day, fabrication and optical behavior remain decoupled during the design phase and numerous assumptions are made about "perfect" geometry. As research moves from theory to real devices, predicting device behavior based on realistic geometry becomes critical. In this dissertation, a set of numerical tools was developed to model micro and nano fabrication processes. They were combined with equally capable tools to model optical performance of the simulated structures. Using these tools, it was predicted and demonstrated that 3D nanostructures may be formed on a standard mask aligner. A space-variant photonic crystal filter was designed and optimized based on a simple fabrication method of etching holes through hetero-structured substrates. It was found that hole taper limited their optical performance and a method was developed to compensate. A method was developed to tune the spectral response of guided-mode resonance filters at the time of fabrication using models of etching and deposition. Auto cloning was modeled and shown that it could be used to form extremely high aspect ratio structures to improve performance of form-birefringent devices. Finally, the numerical tools were applied to metallic photonic crystal devices.

*****

INTRODUCTION

As research moves from theory to real devices, predicting device behavior based on realistic geometry becomes critical [1 7]. Even small distortions can lead to dramatic changes in optical behavior [8]. In this dissertation, a set of numerical tools was developed to model micro and nano fabrication processes. They were combined with equally capable tools to model optical performance of the simulated structures. Using these tools, nano-optical elements were design and optimized by coupling fabrication to optical behavior. Experimental results achieved in the lab verify the concepts developed in this manuscript.Devices used in high speed optical communications networks comprise a wide arrayof material systems [1]. Among the key material systems are silica (both fiber andsilica-on-silicon), silicon oxynitride, sol-gel, dielectric thin film, lithium niobate,galium arsenide, indium phosphide, magneto-optic materials, birefringent crystals,and polymer. Such a wide array of material systems is necessary because of theunique requirements of the constituent passive or active componentry [2]. Passivedevices in integrated optics include simple waveguides, arrayed waveguide gratings,Bragg gratings, thin film filters, and microring resonator filters. Important activeintegrated optical devices include modulators (using electro-optic, acousto-optic,or electro-absoption effects), amplifiers (using heterostructures, quantum wells,or rare-earth doping), and switches (using electro-optic, thermo-optic, electro absorption,or micro-electro-mechanical means). These building-block passiveand active components are fundamental in higher-function devices such as opticaladd/drop multiplexers, interleavers, routers, variable optical attenuators, gainflattening filters, sources, receivers, and detectors.While semiconductor and other inorganic materials have been extensively investigatedand developed during the past decades to meet the demands of high-speedoptical communications and large-scale integrated optical circuits [3], the stringentrequirements of next-generation optical communications networks are pushing thelimits of conventional materials. As a new material available for optical integratedoptics, polymer materials remain among the lesser studied and developed materialsdespite having properties amenable to future requirements. Recently, however,more attention has been given to polymeric materials for use in integrated opticaldevices because of several advantageous features [4]. These features, and manipulationof these features to accomplish feats impossible or not easily achieved with traditional inorganic materials, are the subject of this manuscript.

I. NANO-OPTICAL ELEMENTS

Conventional micro and diffractive optics consists of macroscopic surface-reliefstructures usually designed using scalar methods [9]. Basic passive optical components such aslenses [10-12], prisms [13], and mirrors [14] can be miniaturized and arbitrary shapes realized.These devices have found a host of applications in imaging [15, 16], adaptive optics [17], sensors [18, 19], microscopy [20, 21], communications [22-24], micro-fabrication [2, 5, 6, 25],beam shaping [24], and more. Material properties, however, remain a fundamental limitation. Photonic crystals (PC) are structures with sub-wavelength periodic material propertiesthat can produce sharp electromagnetic resonances. These structures provide a means ofcontrolling and engineering the bulk

electromagnetic properties of materials. Many novel anduseful phenomena have been observed that promise significant impact on future photonicsystems. Useful properties include forbidden transmission [21] and unique dispersive propertieslike negative refractive index [22].

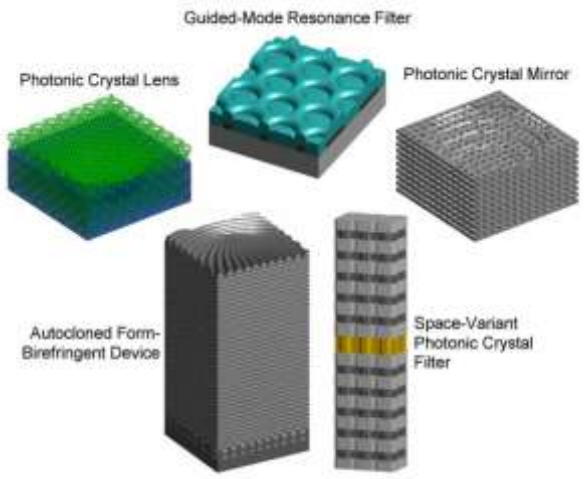

Figure 1: Nano-optical elements

Nano-optical elements combine functionality of micro and diffractive optical elementswith the optical properties of nanophotonic structures like photonic crystals. NOEs can enhanceperformance of devices by providing a means to circumvent fundamental limitations imposed byconventional materials. Concept diagrams of several nano-optical elements are provided inFigure 1. An example simulation is depicted in Figure 2 where a lens has been formed inside a photonic crystal. When light within the photonic band gap is applied, it is completelyreflected. When light from outside the band gap is applied, it is transmitted and focused by thelens. In this manner, multiple functions have been multiplexed into a single device.

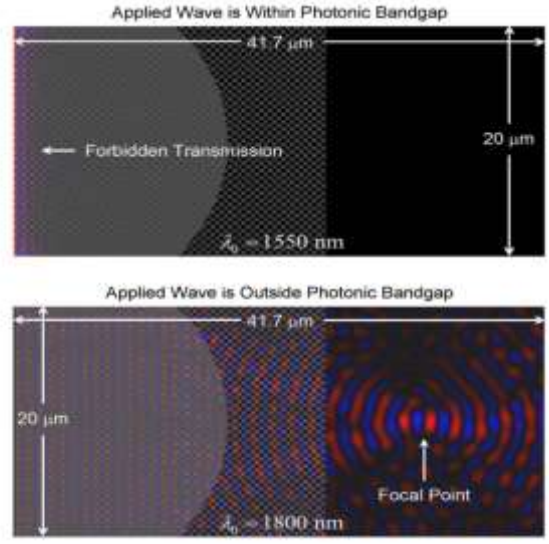

Figure 2: Multifunctional Nano-Optical Element

II. Significance of Nano-Optical Elements

Photonic crystals and other nanophotonic structures hold great promise for manyapplications, and the research community is beginning to integrate them into higher levelsystems like NOEs.NOEs should find a host of applications multiplexing and demultiplexing signals due toinherent spectral filtering properties of photonic crystals,. This could include wavelengthdivision multiplexing (WDM) in fiber optic systems, color filtering in imaging systems, andmore.Devices based on NOEs could be an enabling technology for system miniaturization. Dimensions of optical integrated circuits may be reduced through more efficient routing ofwaveguides using tighter bends and improved crossing. Imaging systems can be made morecompact by replacing complex multi-element lens systems with single element NOEs. Reducingsize and number of components in a system can also lead to improved reliability and lower cost. Display technology may benefit as well. Due to the porous nature of photonic crystals,they can be backfilled with a number of materials with tunable optical properties. Liquid crystalscould tune the index contrast, moving the band gap, and effectively changing color. Sensor technology can exploit highly sensitive optical resonances to detect many things.Chemical sensors could be formed by backfilling with chemically sensitive materials. Highlysensitive acoustic, seismic, pressure, stress, strain, and vibration sensors could be made bydetecting small deformations of the lattice. Imaging systems are likely to benefit from the ability to engineer optical materials.Properties such as negative refractive index could be designed into imaging optics to reduceaberrations. This issue is particularly severe in ultra-miniaturized systems. When more is known about NOEs other applications should become apparent. Thesemay include beam steering, bio-photonics, adaptive optics, and more.

III. Impact of Fabrication on Optical Behavior

Mechanisms causing nano-optical elements to deviate from their “perfect” geometry fallinto two categories. First, random distortions arise from random fluctuations in size, alignment,surface roughness, and other volumetric inhomogeneities. Random distortions are difficult topredict and quantify because simulations are often very large and statistics of the fluctuationsmust be understood. Second, deterministic distortions produce similar effects, but repeatthroughout the element. Deterministic distortions tend to affect optical behavior most severelybecause the same electromagnetic disturbances are encountered many times throughout the entirestructure. Fortunately, these can be predicted by modeling fabrication. Despite this, randomdistortions remain the most heavily studied. As nano-optical elements move from theory topractice, understanding both mechanisms will be critical. For random distortions, the most commonly studied photonic crystal is the stacked-bar, orwoodpile, structure [23, 24]. Two-

dimensional arrays of cylinders [25] and inverse opals [8]have also been studied among others [17]. Width of the photonic band gap seems to be thedominant figure of merit to asses how resilient a photonic crystal is to fluctuations in itsgeometry. Virtually no work can be found on how distortions affect the dispersive behavior ofphotonic crystals. Most literature concludes that fluctuations on the order of 10% to 15% of thelattice constant lead to a 40% to 50% reduction in width of the photonic band gap. A notableexception is the inverse opal, where the band gap resides at much higher frequencies between the8th and 9th bands. For inverse opals, the band gap was found to completely close if fluctuationsexceeded just 2%. Two-dimensional photonic crystals were found to be more sensitive to sizefluctuations than variations in alignment. As may be expected, transverse magnetic (TM) modeswere shown to be more sensitive than transverse electric (TE) modes.Very little work investigating deterministic distortion can be found in the literature.Deformations arising in an autocloning process were addressed in Ref. [19]. This dissertationhas contributed to studies on holographic lithography, NFNP, and more [1-7]. It was shown thatoptical absorption during holographic exposure leads to photonic crystals where fill factor varieswith depth. For negative photoresists like Epon® SU-8 [4], photonic crystals become thinnerwith depth leading to chirped lattices with broadened spectral response. High contrast exposureswere shown to be quite robust to reflections and standing waves during exposure. A face centered-cubicphotonic crystal was able to tolerate 20% reflection from a substrate whilemaintaining similar optical performance. It was shown that performing multiple exposures cansuperimpose different lattices forming hybrids with optical properties of both.Figure 3 compares severity of random and deterministic distortion for one specificphotonic crystal. The lattice is a 2D array of air cylinders in a dielectric medium with εr=12.The leftmost diagram in Figure 3(a) shows the "perfect" photonic crystal with uniform holes,its Brillouin zone, and the photonic band structure for both TE and TM modes. Bands aresymmetric about Γ because the lattice is symmetric through a rotation of 90°. In Figure 3(b)and (c), the lattice is distorted leading to altered band structures. Distorted bands, represented bysolid lines, are compared to bands of the "perfect" photonic crystal, indicated by dashed lines. InFigure 3(b), deterministic distortion is introduced by increasing hole size by 10% of the latticeconstant. Bands of the distorted lattice retain their symmetry, but are offset in frequency withincreasing severity at higher frequencies. A band gap has opened for the TE modes between thefirst and second bands. The TM band gap has shifted by around 30% to higher frequencies andis wider. In Figure 3(c), random distortion is introduced by randomly varying hole size by20% of the lattice constant. It is immediately obvious how less the bands are affected by randomfluctuations. This is partially due to overall average refractive index remaining the same. Forpurely random variations, bands should retain their symmetry. The small degree of asymmetryobserved in this example is attributed to a slight anisotropy of the supercell used in thecalculation, so it is a purely numerical artifact. It should be noted that while random distortion isvisually most dramatic, it is the more subtle deterministic distortion that is most serious. For thisreason, it is important to predict optical behavior of nano-optical elements based on realisticgeometry.

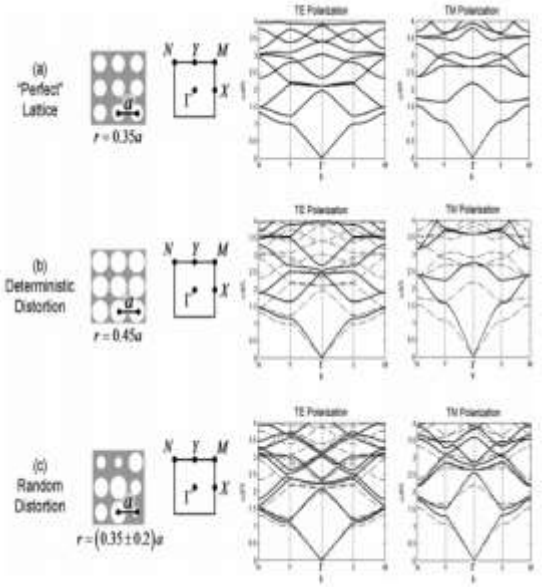

Figure 3: Comparison between random and deterministic distortion

To demonstrate the impact of realistic geometry on a real structure, reflection from twoface-centered-cubic photonic crystals are compared in Figure 4. A depiction of the unit cellsare shown at the left side of the diagram. The "perfect" geometry is rendered in blue, while amore realistic geometry resulting from holographic lithography is rendered in red. Reflectionfrom a ten layer slab from both lattices are compared at the right side of the diagram. Width ofthe band gap is slightly wider for the realistic case and red-shifted to a longer wavelength. Peakreflection of the realistic structure is lower. A kink observed in the spectrum of the realisticphotonic crystal suggests there is interesting dispersive behavior that is completely missed whenperfect geometry is assumed.

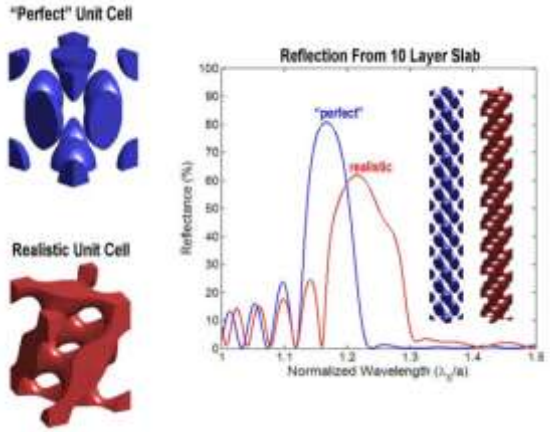

Figure 4: Comparison of "perfect" and realistic FCC photonic crystal

IV. General Considerations for Numerical Modeling

To predict geometry of NOEs, key steps in fabrication must be identified and modeled accurately. A background in suitable numerical methods is helpful. It is best to seek techniques capable of handling large scale problems with high volumetric complexity since realistic devices are rarely comprised of perfect geometric patterns and can be quite large in terms of the optical wavelengths of interest. For electromagnetic simulations, finite-element methods [10] and finite-difference methods [11-17] are attractive, particularly when metals are incorporated. For 2D simulations, the finite-difference frequency-domain (FDFD) method is accurate, simple to implement, and excellent for modeling complex structures of finite size [5, 6]. The transfer matrix method [2, 8] is popular for 2D and 3D structures, especially when they contain metals. For layered and periodic dielectric devices with moderate to low index contrast, rigorous coupled-wave analysis (RCWA) [9-12] is very fast and efficient. Finite-difference time-domain (FDTD) [3, 4] remains a very powerful tool for modeling finite sized devices, large scale structures, and characterizing devices over very broad frequency range. FDTD has difficulty resolving sharp resonances or any abrupt change in spectral response, but it is exceptionally capable of identifying if resonances are present and locating their position in frequency

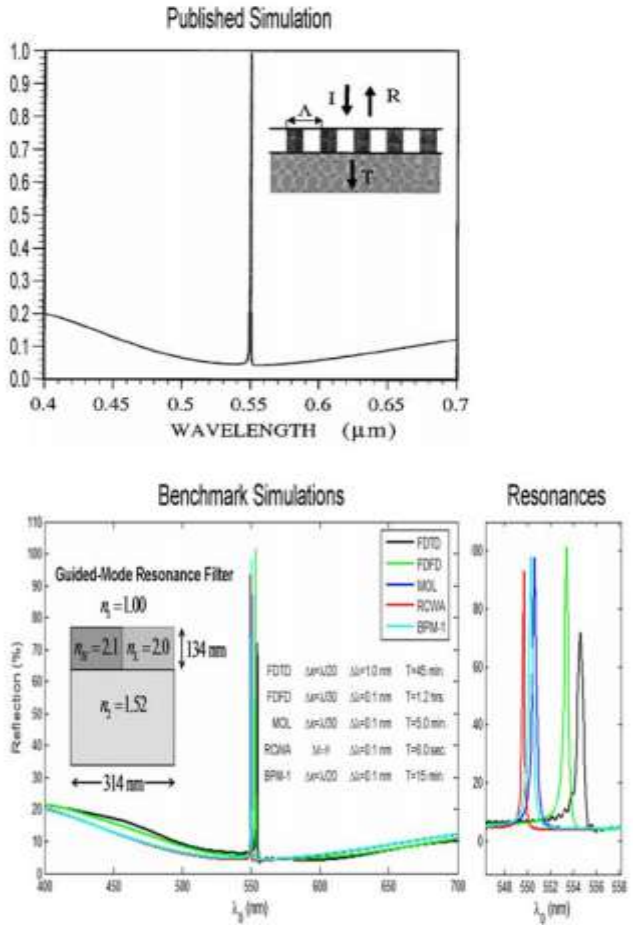

Figure 5: Benchmark Simulations for EM Simulation Tools

Figure 5 compares theoretical results obtained in Ref. [13] to benchmark simulations for all electromagnetic simulation tools outlined in this dissertation. Numerical resolution, spectral resolution, and simulation time is summarized in this figure. A close-up of the simulated resonances is provided in the bottom right diagram. Numerical dispersion has shifted the resonance peaks to slightly longer wavelengths in the models employing finite-differences.Etching, developing, and deposition processes can be modeled by tracking progression of a surface. There are four popular approaches found in literature. These are string methods [9, 4, 5], cell volume methods [3, 6-10], level set methods (LSM) [1-3], and fast marching methods (FMM) [13]. String, or marker particle, methods resolve the surface with a number of discrete points. During simulation, position of each point is updated based on position of surrounding points and a local rate function. These methods are very fast and efficient when surface topology is simple, smooth, and continuous. This is the case for much of grayscale lithography and analog devices. When structures are complex with detached surfaces and sharp bends, the method can become unstable and is difficult to implement. For these reasons, the string method is mostly limited to 2D problems. Cell volume methods represent bulk materials as an array of cube shaped cells. Each cell is assigned a fictitious volume that is adjusted as the surface progresses. Cells with zero volume represent points where the bulk material does not exist. Cells where the volume is filled represent points where the bulk material is present. Cells with partially filled volumes interpolate position of the surface. The main trick implementing these methods is modifying how cell volume is reduced based on the direction the surface is moving through the cell. This is a difficult calculation in the cell volume framework and fine grids are needed to obtain accurate results. For this reason, cell volume methods require large amounts of memory and run slower than string methods, but are able to handle arbitrarily complex surfaces and extend well to three dimensions. Of all techniques, LSM and FMM seem to offer the greatest compromise between speed, flexibility, and efficiency while being able handle very complex geometries. Level set methods may be the most generalized and most rigorous technique for modeling evolution of surfaces.They are best tailored for modeling etching and deposition due to the bidirectional nature of the surface and surface dependent growth rates encountered in the process. Fast marching methods are incredibly fast and accurate algorithms best suited to model processes like developing where surfaces progress in only one direction and rate depends only on position. Both LSM and FMM offer much simpler means of calculating geometric properties of the surface such as surface normal and curvature.

V. MAXWELL'S EQUATIONS AND THEOREMS

Maxwell's equations are the fundamental laws that govern behavior of all electromagnetic energy. They are based on a macroscopic view of how waves interact with matter and may take many forms. To understand optical behavior in nano-optical elements, it is necessary to have an understanding of Maxwell's

Table 1: Maxwell's Equations

Integral Form	Differential Form	Description	
$\oiint_S \vec{D}(t)\cdot d\vec{S} = \int_V \rho_v(t)\,dv$	$\nabla\cdot\vec{D}(t) = \rho_v(t)$	Gauss' law	Time-Domain
$\oiint_S \vec{B}(t)\cdot d\vec{S} = 0$	$\nabla\cdot\vec{B}(t) = 0$	No magnetic charge	
$\oint_L \vec{E}(t)\cdot d\vec{L} = -\frac{\partial}{\partial t}\iint_S \vec{B}(t)\cdot d\vec{S}$	$\nabla\times\vec{E}(t) = -\frac{\partial\vec{B}(t)}{\partial t}$	Faraday's law	
$\oint_L \vec{H}(t)\cdot d\vec{L} = \iint_S \left[\vec{J}(t) + \frac{\partial\vec{D}(t)}{\partial t}\right]\cdot d\vec{S}$	$\nabla\times\vec{H}(t) = \vec{J}(t) + \frac{\partial\vec{D}(t)}{\partial t}$	Ampere's circuit law	
$\vec{D}(t) = \bar{\varepsilon}(t) * \vec{E}(t)$	$\vec{B}(t) = \bar{\mu}(t) * \vec{H}(t)$		
$\oiint_S \vec{D}\cdot d\vec{S} = \int_V \rho_v dv$	$\nabla\cdot\vec{D} = \rho_v$	Gauss' law	Frequency-Domain
$\oiint_S \vec{B}\cdot d\vec{S} = 0$	$\nabla\cdot\vec{B} = 0$	No magnetic charge	
$\oint_L \vec{E}\cdot d\vec{L} = -j\omega\iint_S \vec{B}\cdot d\vec{S}$	$\nabla\times\vec{E} = -j\omega\vec{B}$	Faraday's law	
$\oint_L \vec{H}\cdot d\vec{L} = \iint_S \left(\vec{J} + j\omega\vec{D}\right)\cdot d\vec{S}$	$\nabla\times\vec{H} = \vec{J} + j\omega\vec{D}$	Ampere's circuit law	
$\vec{D} = \bar{\varepsilon}\vec{E}$	$\vec{B} = \bar{\mu}\vec{H}$		

equations and how they are applied. A summary of Maxwell's equations is provided in Table 1.

A. Time-Domain Form

The most widely used form of Maxwell's equations are differential equations, as opposed to integral equations. In time-domain form [24], these are:

$$\nabla\cdot\vec{D}(t) = \rho_v(t) \quad (1)$$

$$\nabla\cdot\vec{B}(t) = 0 \quad (2)$$

$$\nabla x\,\vec{E}(t) = \frac{\partial\vec{B}(t)}{\partial t} \quad (3)$$

$$\nabla x\,\vec{H}(t) = \vec{J} + \frac{\partial\vec{D}(t)}{\partial t} \quad (4)$$

The field parameters $\vec{D}, \vec{B}, \vec{E}$ and $\vec{E}$ represent electric flux density (C/m2), electric field intensity (V/m), magnetic flux density (W/m2), and magnetic field intensity (A/m) respectively. Electric charge density ρv (C/m3) and electric current density J G (A/m2) represent sources that can induce electromagnetic fields or be induced by the fields.All materials are comprised of charged particles that are displaced in the presence of an applied electric field. Accelerating charges radiate fields that combine out of phase with the applied wave. The overall effect is to modify propagation so waves behave differently than they would in a vacuum. To incorporate these effects in a simplified manner, they are treated macroscopically through the constitutive parameters $\bar{\varepsilon}$ (t),μ(t) , and sometimes σ(t). In general, these are time-varying tensor quantities that relate to the fields through the following equations that involve convolutions.

$$\vec{D}(t) = \bar{\varepsilon}(t) * \vec{E}(t) \quad (5)$$

$$\vec{B}(t)=\bar{\mu}(t)*\vec{H}(t) \quad (6)$$

$$\vec{J}(t)=\bar{\sigma}(t)*\vec{E}(t) \quad (7)$$

The dielectric permittivity $\bar{\varepsilon}$ characterizes how well a material can store energy imposed by an electric field. Permeability $\bar{\mu}$ quantifies how efficiently energy is stored due to an applied magnetic field. The conductivity $\bar{\sigma}$ arises from free charges that form electrical currents in the presence of an applied electric field.

B. ***Frequency-Domain Form***

Transforming Eqs. (1) - (7) to the frequency-domain simplifies the mathematical framework by reducing convolutions to simple products.

$$\nabla \bullet \vec{D} = \rho_v \quad (8)$$

$$\nabla \bullet \vec{B} = 0 \quad (9)$$

$$\nabla \times \vec{E} = -j\omega\vec{B} \quad (10)$$

$$\nabla \times \vec{H} = \vec{J} + j\omega\vec{D} \quad (11)$$

$$\vec{D} = \bar{\varepsilon}\vec{E} \quad (12)$$

$$\vec{B} = \bar{\mu}\vec{H} \quad (13)$$

$$\vec{J} = \bar{\sigma}\vec{E} \quad (14)$$

In this form, it is possible to eliminate the terms $\vec{D}, \vec{B} and \vec{J}$ from Maxwell's equations.

$$\nabla \bullet \left(\bar{\varepsilon}\vec{E}\right) = q \quad (15)$$

$$\nabla \bullet \left(\bar{\mu}\vec{H}\right) = 0 \quad (16)$$

$$\nabla \times \vec{E} = -j\omega\bar{\mu}\vec{H} \quad (17)$$

$$\nabla \times \vec{H} = \bar{\sigma}\vec{E} + j\omega\bar{\varepsilon}\vec{E} \quad (18)$$

Most often permittivity and permeability are not tensor quantities. In addition, charge $\rho_v$is usually ignored and conductivity is incorporated into a complex permittivity term. Under these conditions, Maxwell's equations assume their most familiar form.

$$\nabla \bullet \left(\varepsilon\vec{E}\right) = 0 \quad (19)$$

$$\nabla \bullet \left(\mu\vec{H}\right) = 0 \quad (20)$$

$$\nabla \times \vec{E} = -j\omega\mu\vec{H} \quad (21)$$

$$\nabla \times \vec{H} = j\omega\varepsilon\vec{E} \quad (22)$$

C. Wave Equations

Perhaps the most significant aspect of Maxwell's equations is that they predict propagating waves. The curl equations show that time changing electric fields induce curling, or circulating, magnetic fields in the immediate vicinity. Likewise, time changing magnetic fields induce circulating electric fields. In this manner, oscillating fields continue to induce other oscillating fields and a wave is formed. To better understand the wave phenomenon, it makes sense to combine Maxwell's curl equations since it is the interaction of these two equations that predicts propagation. The combined equation is called a "wave equation" and it is possible to derive it in terms of just the magnetic field or just the electric field. Wave equations enable fully rigorous analysis of electromagnetic problems using a single equation while incorporating all information from both of Maxwell's curl equations. To begin deriving full vector wave equations, Eqs. (21) and (22) are written as

$$(1/\mu)\nabla \times \vec{E} = -j\omega\vec{H} \quad (23)$$

$$(1/\varepsilon)\nabla \times \vec{H} = j\omega\vec{E} \quad (24)$$

Taking the curl of these equations leads to:

$$\nabla \times (1/\mu)\nabla \times \vec{E} = -j\omega\left(\nabla \times \vec{H}\right) \quad (25)$$

$$\nabla \times (1/\varepsilon)\nabla \times \vec{H} = j\omega\left(\nabla \times \vec{E}\right) \quad (26)$$

The curl operations on the right side of these equations can be replaced using the original curl equations. This leads to the full vector wave equations.

$$\nabla \times \frac{1}{\mu}\nabla \times \vec{E} = \omega^2\varepsilon\vec{E} \quad (27)$$

$$\nabla \times \frac{1}{\varepsilon}\nabla \times \vec{H} = \omega^2\mu\vec{H} \quad (28)$$

The wave equations can be written in terms of the free space wave number k_0, where $k_0 = \omega/c$.

$$\nabla \times \frac{1}{\mu_r}\nabla \times \vec{E} = k_0^2\varepsilon_r\vec{E} \quad (29)$$

$$\nabla \times \frac{1}{\varepsilon_r}\nabla \times \vec{H} = k_0^2\mu_r\vec{H} \quad (30)$$

VI. CONCLUSION

This manuscript designed and optimized several nano-optical elements by considering how fabrication affects their optical behavior. Background was given to understand device theory. Numerical tools were discussed and detailed formulations were provided for each along with block diagrams

summarizing their implementation. To better understand electromagnetic theory of nano-optical elements and concepts used to develop numerical models, background information was provided to introduce Maxwell's equations from which wave equations were derived. These were used to explain scaling theories and introduce the concept of left-handed materials.Microscopic models of the response of materials were presented in the form of the Lorentz oscillator model for dielectrics and the Drude model to metals. From these, basic properties of bulk optical materials were identified and described.

REFERENCES

[1] R. Rumpf and E. G. Johnson, "Fully three-dimensional modeling of the fabrication and behavior of photonic crystals formed by holographic lithography," Journal of the Optical Society of America A, vol. 21, pp. 1703-1713, 2004.

[2] R. C. Rumpf and E. G. Johnson, "Modeling the formation of photonic crystals by holographic lithography," presented at Proceedings of SPIE Micromachining Technology for Micro-Optics and Nano-optics III, Bellingham, WA, 2005.

[3] P. Srinivasan, R. C. Rumpf, and E. G. Johnson, "Fabrication of 3-D photonic crystals by two-step dry etching of layered media," presented at SPIE Micromachining Technology for Micro-Optics and Nano-Optics IV, San Jose, CA, 2006.

[4] Z. Li and X. Zhang, "Fragility of photonic band gaps in inverse-opal photonic crystals," Phys. Rev. B, vol. 62, pp. 1516-1519, 2000.

[5] H. P. Herzig, Micro-optics: Elements, systems and applications. Philadelphia: Taylor &Francis Inc., 1998.

[6] D. L. Dickensheets, "Imaging performance of off-axis planar diffractive lenses," J. Opt. Soc. Am. A, vol. 13, pp. 1849-1858, 1996.

[7] K. Yamada, W. Watanabe, Y. Li, and K. Itoh, "Multilevel phase-type diffractive lenses in silica glass induced by filamentation of femtosecond laser pulses," Opt. Lett., vol. 29, pp. 1846-1848, 2004.

[8] C. Gimkiewicz, D. Hagedorn, J. Jahns, E. B. Kley, and F. Thoma, "Fabrication of microprisms for planar optical interconnections by use of analog gray-scale lithography with high-energy-beam-sensitive glass," Applied Optics, vol. 38, pp. 2986-2990, 1999.J.L. Vossen: *Thin Film Processes* (Academic, New York 1976) 8.9 M. Gad-el-Hak (Ed.): *The MEMS Handbook* (CRC, Boca Raton 2002)

[9] J. M. Bendickson, E. N. Glytsis, and T. K. Gaylord, "Metallic surface-relief on-axis and off-axis focusing diffractive cylindrical mirrors," J. Opt. Soc. Am. A, vol. 16, pp. 113- 130, 1999.

[10] G.T.A. Kovacs: *Micromachined Transducers Sourcebook* (McGraw Hill, New York 1998)P. Rai-Choudhury (Ed.): *Handbook of Microlithography, Micromachining and Microfabrication. Vol.2: Micromachining and Microfabrication*(SPIE/IEE, Bellingham, Washington/London 1997)

[11] J. Rasanen and K. E. Peiponen, "On-line measurement of the thickness and optical quality of float glass with a sensor based on a diffractive element," Appl. Opt., vol. 40, pp. 5034-5039, 2001.

[12] S. P. Simonaho and R. Silvennoinen, "Sensing of wood density by laser light scattering pattern and diffractive optical element based sensor," J. Opt. Technol., vol. 73, pp. 170- 174, 2006.

[13] V. Emiliani, D. Cojoc, E. Ferrari, V. Garbin, C. Durieux, M. Coppey-Moisan, and E. D. Fabrizio, "Wave front engineering for microscopy of living cells," Opt. Exp., vol. 13, pp. 1395-1405, 2005.

[14] E. D. Fabrizio, D. Cojoc, and S. Cabrini, "Diffractive optical elements for differential interference contrast x-ray microscopy," Opt. Exp., vol. 11, pp. 2278-2288, 2003.

[15] F. Niklaus, P. Enoksson, E. Kalveston, G. Stemme: Void-free full-wafer adhesive bonding, J. Micromech. Microeng. 11, 100–107 (2000)

[16] Y. Orihara, W. Klaus, M. Fujino, and K. Kodate, "Optimization and application of hybrid-level binary zone plates," Appl. Opt., vol. 40, pp. 5877-5885, 2001.

[17] W.H. Ko, J.T. Suminto, G.J. Yeh: Bonding techniques for microsensors. In: *Micromachining andMicropackaging for Transducers*, ed. by W.H. Ko (Elsevier, Amsterdam 1985)

[18] H. Sasaki, I. Fukuzaki, Y. Katsuki, and T. Kamijoh, "Design considerations of stacked multilayers of diffractive optical elements for optical network units in optical subscribernetwork applications," Appl. Opt., vol. 37, pp. 3735-3745, 1998.

[19] S. Jeon, G. P. Wiederrecht, and J. A. Rogers, "Photonic systems formed by proximity field nanopatterning," Proceedings of the SPIE on Micromachining Technology for Micro-Optics and Nano-Optics III, vol. 5720, pp. 187-195, 2005.

[20] W. S. Mohammed, A. Mehta, M. Pitchumani, and E. G. Johnson, "Selective Excitation of the TE01 Mode in Hollow-Glass Waveguide Using a Subwavelength Grating," IEEE Phot. Tech. Lett., vol. 17, pp. 1441-1443, 2005.

[21] A. Schilling, H. P. Herzig, L. Stauffer, U. Vokinger, and M. Rossi, "Efficient beam shaping of linear, high-power diode lasers by use of micro-optics," Appl. Opt., vol. 40, pp. 5852-5859, 2001.

[22] M. R. Wang and X. G. Huang, "Subwavelength-resolvable focused non-Gaussian beam shaped with a binary diffractive optical element," Appl. Opt., vol. 38, pp. 2171-2176, 1999.

[23] Y. Zhao, Y. P. Li, and Q. G. Zhou, "Vector iterative algorithm for the design ofdiffractive optical elements applied to uniform illumination," Opt. Lett., vol. 29, pp. 664-666, 2004.

[24] A. Chutinan and S. Noda, "Effects of structural fluctuations on the photonic band gap during fabrication of a photonic crystal: a study of a photonic crystal with a finite number of periods," J. Opt. Soc. Am. B, vol. 16, pp. 1398-1402, 1999.

Nadeem Khargan Alhareeb was born in Nasiriyiahcity,Thi-Qar province, Iraq, on November 1981. Received his B.S. degrees in Electrical Engineering from Al Mustansiriyah University, Baghdad ,Iraq, in 2007. Received his M.SC degree in the department of Communication Engineering. Currently; he become as a Lecturer in Biomedical Engineering department, university of ThiQar, Iraq